Apolipoprotein AI Deficiency Inhibits Serum Opacity Factor Activity against Plasma High Density Lipoprotein via a Stabilization Mechanism

ARTICLE *in* BIOCHEMISTRY · MARCH 2015

Impact Factor: 3.02 · DOI: 10.1021/bi501486z · Source: PubMed

Apolipoprotein AI Deficiency Inhibits Serum Opacity Factor Activity against Plasma High Density Lipoprotein via a Stabilization Mechanism.

Corina Rosales, [1] Niket Patel,[1] Baiba K. Gillard,[1] Dedipya Yelamanchili,[1] Yaliu Yang,[1] Harry S. Courtney,[2] Raul D. Santos,[3] Antonio M. Gotto, Jr.,[1] and Henry J. Pownall[1,4]

[1]Laboratory of Atherosclerosis and Lipoprotein Research, Department of Cardiology, Houston Methodist Research Institute, 6670 Bertner Avenue, Houston TX 77030 , Weill Cornell Medical College, 1305 York Ave, New York, NY, 10021 and [2]Veterans Affairs Medical Center and Department of Medicine, University of Tennessee Health Science Center, Memphis, TN 38104. [3]Heart Institute-INCOR-University of Sao Paulo Sao Paulo, BR

[4]Corresponding author: Email: HJPownall@HoustonMethodist.org

Abstract

The reaction of Streptococcal serum opacity factor (SOF) against plasma high-density lipoproteins (HDL) produces a large cholesteryl ester-rich microemulsion (CERM), a smaller neo HDL that is apolipoprotein (apo) AI-poor, and lipid-free apo AI. SOF is active vs. both human and mouse plasma HDL. In vivo injection of SOF into mice reduces plasma cholesterol ~40% in 3 hours while forming the same products observed in vitro, but at different ratios. Previous studies supported the hypothesis that labile apo AI is required for the SOF reaction vs. HDL. Here we further tested that hypothesis by studies of SOF against HDL from apo AI-null mice. When injected into apo AI-null mice, SOF reduced plasma cholesterol ~35% in three hours. The reaction of SOF vs. apo AI-null HDL in vitro produced a CERM and neo HDL, but no lipid-free apo. Moreover, according to the rate of CERM formation, the extent and rate of the SOF reaction vs. apo AI-null mouse HDL was less than that against wild-type (WT) mouse HDL. Chaotropic perturbation studies using guanidine hydrochloride showed that apo AI-null HDL was more stable than WT HDL. Human apo AI added to apo AI-null HDL was quantitatively incorporated, giving reconstituted HDL. Both SOF and guanidine hydrochloride displaced apo AI from the reconstituted HDL. These results support the conclusion that apo AI-null HDL is more stable than WT HDL because it lacks apo AI, a labile protein that is readily displaced by physico-chemical and biochemical perturbations. Thus, apo AI-null HDL is less SOF-reactive than WT HDL. The properties of apo AI-null HDL can be partially restored to those of WT HDL by the spontaneous incorporation of human apo AI. It remains to be determined what other HDL functions are affected by apo AI deletion.

Human plasma high-density lipoprotein-cholesterol (HDL-C) concentrations are a negative risk factor for cardiovascular disease (CVD),(*1, 2*) and their elevation via pharmacological measures reduces incident CVD.(*3, 4*) However, HDL-C concentrations may not be as reliable a predictor of CVD as once thought: one study showed that controlling for apolipoprotein (apo) AI inverted the negative relationship of HDL-C with pre-clinical atherosclerosis,(*5*) so apo AI may be the dominant determinant of reduced CVD in subjects with elevated HDL-C concentrations. Apo AI is the major HDL protein (65%),(*6*) and its deficiency is associated with low HDL-C, planar xanthomas, reduced plasma apo E, and premature CVD in humans.(*7, 8*) In contrast, apo AI-deficiency in mice is associated with low HDL-C but not with increased susceptibility to atherosclerosis, an observation that may be a function of elevated HDL-apo E in apo AI-deficient mice.(*9, 10*) Apo AI has other salutary effects: apo AI profoundly reverses rheumatoid arthritis in a rat model and is a component of the human trypanocidal HDL fraction that prevents some strains of African sleeping sickness in humans.(*11, 12*)

Several studies, though somewhat conflicting, show that, as a component of atheroprotection, HDL function is more important than plasma HDL-C concentration. A likely determinant of HDL function is its unusual thermodynamic properties: several studies support a model of HDL residing in a kinetic trap, so that when challenged by various physical perturbations HDL disproportionates into fused particles and lipid-free (LF) apo AI.(*13-15*) Several plasma activities relevant to HDL metabolism also disrupt HDL structure—hepatic lipase,(*16, 17*) cholesteryl ester transfer protein,(*18*) lecithin:cholesterol acyltransferase,(*19*) phospholipid transfer protein,(*20, 21*) and especially Streptococcal serum opacity factor (SOF), which at low doses (1 μg/mL) disrupts HDL structure in vitro(*22*) and reduces plasma cholesterol ~43% in 3 hours in wild-type (WT) mice.(*23*) Previous studies supported the hypothesis that SOF activity against HDL required labile apo AI, a hallmark of HDL instability.(*24*) We have now further tested that hypothesis by quantifying SOF activity against HDL from apo AI-null mice and comparing the stability of WT and apo AI-null mouse HDL by chaotropic perturbation with guanidine hydrochloride (GdmCl).

Experimental Procedures (Materials and Methods)

Materials: The total lipoproteins (TLP) were isolated by flotation of plasma from a previously characterized Brazilian patient with total apo AI deficiency, which was associated with a plasma HDL-C concentration that was 10% of normal.(*8*) One TLP aliquot (200 μg/mL in 200 μL) was analyzed by SEC; another was incubated at 37 °C overnight with SOF (1 μg) and also analyzed by SEC. HDL from WT and apo AI-null mice on a C57Bl/6 background (Jackson Laboratories) were isolated by sequential ultracentrifugal flotation at d = 1.063 and 1.21 g/mL. Apo AI-null HDL was reconstituted to a "native" HDL by the titrated addition of human apo AI and isolated by size exclusion chromatography (SEC).

An active truncated fragment of SOF with opacification activity was purified as previously described.(*25*)

All animal procedures were carried out under approval from the institutional animal care and use committee.

Mouse Plasma Cholesterol Decay Kinetics: SOF or saline were injected via the tail-vein into mice. At various post injection times the mice were euthanized and their blood collected by heart puncture into EDTA vacutainer tubes and transferred to wet ice. Plasma was separated from the cells by low speed centrifugation at 4 °C and the total plasma cholesterol determined. Plasma cholesterol concentrations at

each time point are the means of ≥3 and ≥7 samples for SOF injections into apo AI-null and WT mice, respectively, except for t = 0, for which n = 9.

SOF Reaction Kinetics: The rate of change in right angle light scattering was used to follow the course of the SOF reaction in real time.(*22*) This assay follows the formation of one of the SOF reaction products, the cholesteryl ester (CE) microemulsion (CERM), which scatters light, because of its large dimension (~500 nm). Excitation and detection were both at 325 nm. Kinetic parameters were extracted by fitting the data to a growing exponential curve using Sigma Plot Software (Systat Software, Inc.). The SOF reaction was also followed by measuring the distribution of products by SEC over two Superose HR6 columns in tandem. Kinetic experiments were conducted similarly with HDL from apo AI-null mice, which was reconstituted with human apo AI.

Chaotropic Perturbation (CP): Ultracentrifugally isolated HDL from WT and apo AI-null mice was further purified by SEC over Superose HR6 as previously described.(*26*) HDL stability was determined by incubating apo AI-null or WT HDL (0.11 mg/mL and 0.4 mg/mL respectively) for 22 hours with various concentrations of GdmCl and analyzing by SEC as previously reported.(*15*)

CP was also conducted with apo AI-null HDL reconstituted with human apo AI. Human apo AI (0.133 mL at 0.2 mg/mL) was added to 0.4 mL apo AI-null HDL (0.6 mg/mL), incubated at room temperature for 3 hours, and stored at 4 °C overnight. Various concentrations of GdmCl (0.5, 1, 2, and 3 M) were added, incubated at room temperature for 22 hours, and analyzed by SEC.

Effects of SOF on Reconstituted HDL: HDL was isolated from plasma of apo AI-null mice and split into three 0.15 mL aliquots (0.6 mg/mL). The first, a control, was analyzed by SEC. Human apo AI (0.05 mL at 0.2 mg/mL) was added to the other two aliquots and incubated for 3 hours at room temperature; one aliquot was then analyzed by SEC. SOF (1.3 μg) was added to the third aliquot and incubated overnight at 37 °C, after which it was also analyzed by SEC.

Compositional Analyses: Apo AI-null HDL, with and without SOF treatment, were analyzed for protein using the BioRad DC protein kit. HDL-triglyceride (TG), cholesteryl esters, free cholesterol, and phospholipids (PL) were determined using kits and standards from Wako. The apo compositions of HDL and the SOF reaction products were determined by SDS-PAGE and visualized on a BioRad Gel Doc EZ Imager after staining with Coomassie Blue and by immunoblotting for apos AI, AII, and E.

Statistical Analysis: All values are expressed as mean ± SEM. Data were compared using ANOVA followed by Student's t-test for pair-wise comparisons between SOF-treated and saline-treated groups. Values of $p < 0.05$ were considered statistically significant. Statistical analysis and calculation of regression curves was performed using SigmaPlot 11.2 (Systat Software, Inc.). Rate constants were calculated from regression fits of the data points vs. time.

Results

Effects of SOF on TLP from an Apo AI-Deficient Patient: Treatment of normal human plasma HDL or HDL with SOF produces a CERM, which elutes in the void volume, a small HDL eluting at ~32 mL that we that we previously called neo HDL, and lipid free apo AI, which elutes at ~34 mL.(*22*) We thus tested the effects of SOF on TLP from a normal volunteer with those of a patient with total apo AI deficiency. The SEC profile of normal plasma TLP (**Figure 1 A**) shows prominent peaks for VLDL, LDL, and HDL. Incubation of normal plasma TLP with SOF produced the previously reported CERM in the void volume, (15 mL), the neo HDL (32 mL), and lipid-free apo AI (34 mL);(*22*) the SEC also shows that the peak for

LDL is shifted to slightly earlier elution volumes corresponding to a larger particle; the difference between the SEC for TLP with and without SOF incubation (dashed line) is large and due to CERM formation (**Figure 1 B**).

The SEC profile of the TLP from the patient (**Figure 1 C**) also showed prominent peaks for VLDL, LDL, and HDL; relative to the other peaks, the peak for HDL is a smaller than that observed for normal TLP. A peak eluting at 20 mL corresponds to the elution volume of intermediate density lipoproteins (IDL). As with LDL in normal TLP, SOF induced a small shift to an earlier elution time for IDL and LDL. The peak in the void volume doubled in size after SOF incubation and the double peak for HDL was replaced by a single peak eluting later; we previously attributed this peak to neo HDL.(*22*) Given the equal loading of the SEC columns for TLP ± SOF and noting that the magnitudes of the IDL and LDL peaks were the same in **Figure 1 C** and **D**, we calculated the difference to obtain a "CERM" peak (**Figure 1 D**, dashed curve). This CERM peak is much smaller than that formed from normal HDL. These data suggest that SOF reacts with the HDL from apo AI-deficient plasma, thereby rationalizing more detailed studies in apo AI-null mice that can be tested in vitro and in vivo.

SOF is Less Hypocholesterolemic in Apo AI-Null vs. WT Mice: SOF reduces plasma cholesterol in mice by transferring most of the HDL-CE to a CERM that contains apo E and is cleared by hepatic LDL-receptors. The SOF reaction is associated with the production of LF apo AI in vitro and seems to be dependent on HDL stability and apo AI lability. Moreover, replacement of apo AI with apo AII, which is more lipophilic than apo AI, reduces the rate and magnitude of opacification.(*26*) Thus, we tested the effects of apo AI deficiency on the kinetics of cholesterol clearance in apo AI-null mice. Our data confirmed a previous report(*27*) that apo AI-null mice have lower plasma total cholesterol than WT mice (data not shown); before SOF injection, the mean plasma cholesterol concentration for our apo AI-null mice was 45.9 ± 1.9 mg/dL (**Figure 2**). Following SOF injection, the plasma cholesterol in the mice decreased to 28.9 ± 2.7 mg/dL at 8 h; this decrease led to cholesterol concentrations significantly different from the initial plasma cholesterol concentration and the concentration in the saline group at the same time point (**Figure 2**). Comparison of the regression curves for the SOF-mediated decrease in plasma cholesterol concentrations in WT(*22*) and apo AI-null mice (this study) showed that the reductions of plasma cholesterol at 3 hours were 37 and 15 mg/dL, respectively; comparison on the basis of the initial plasma cholesterol concentrations gave similar percent decreases in plasma cholesterol concentrations.

SOF Disrupts Apo AI-null HDL: According to SEC, apo AI-null HDL elutes as a single broad peak with a peak elution volume similar to those of human(*22*) and WT mouse HDL (**Figure 3 A**). After incubation with SOF, the single peak for HDL is replaced by a peak that elutes in the void volume (CERM) and a pair of overlapping peaks corresponding to larger and smaller neo HDL, centered on the peak position of the original apo AI-null HDL (**Figure 3 B**). As previously designated,(*22*) according to their compositions, we denote the early eluting peak as CERM and the late eluting peaks as neo HDL. Notably, and unlike the reaction of SOF against WT mouse and native human HDL, there is no LF protein eluting after the peaks in the HDL region (LF Apo AI elution volume = 34 mL). SDS-PAGE revealed that the starting HDL, as expected, contains no apo AI but has prominent bands for apo E and apo AII (**Figure 3 C**). These findings were confirmed by immunoblotting for apo AI, apo E and apo AII (**Figure 3 D—F**). Of note is that the larger neo HDL has relatively higher apo E while the smaller neo HDL has higher apo AII. As with SOF action on human HDL and WT mouse HDL, apo E was detected in the CERM peak.(*22, 23*)

As with the reaction of SOF against human HDL, SOF-catalyzed the disproportionation of apo AI-null mouse HDL into CERM and neo HDL in a way that transferred the major nonpolar components, mostly CE, to the CERM and the polar components, protein and phospholipid, to neo HDL (**Figure 4**). The composition of apo AI-null mouse HDL is different from that of human HDL, and these differences are reflected in the compositions of the reaction products. Human HDL contains more protein and TG but less phospholipid and cholesteryl ester than apo AI-null mouse HDL (**Figure 4**). Given that most neutral lipids are transferred to the CERM, the CERM formed from apo AI-null mouse HDL is also more CE-rich than the CERM formed from human HDL. In contrast, the apo AI-null neo HDL is more protein-rich but phospholipid-poor than the neo HDL formed from human HDL.

Apo AI-null vs. WT HDL is Less SOF-Reactive and More Stable: The reactions of SOF against apo AI-null HDL and WT mouse HDL were compared by kinetic turbidimetry (**Figure 5**). The magnitude of the maximum light scattering (I_{max}) is proportional to the amount of the major light scattering product formed, the CERM. Our data showed that I_{max} for the reaction of SOF against WT mouse HDL is ~5 times that observed with apo AI-null HDL. In addition, the SOF reaction rate vs. WT mouse HDL is ~4 times faster than that observed against apo AI-null mouse HDL.

Reconstitution of Apo AI-null HDL with Human Apo AI Normalizes SOF Reactivity: The effects of SOF on apo AI-null HDL reconstituted with human apo AI were tested. According to SEC, apo AI elutes at ~34 mL (**Figure 6 A)** and apo AI-null HDL elutes broadly between 24 and 31 mL (**Figure 6 B)**. SEC of apo AI-null HDL to which human apo AI has been added showed the absence of the apo AI peak at ~34 mL and a peak for HDL that was minimally changed, indicating incorporation of apo AI into the apo AI null HDL (**Figure 6 C)**. Incubation of SOF with the human apo AI-reconstituted apo AI-null HDL showed a large peak in the void volume, CERM, and a shift of the HDL to later elution volumes with peaks at 31 and 34 mL (**Figure 6 D)**, which respectively correspond to the elution volumes of neo HDL formed from mouse(*26*) and human HDL(*22*) and apo AI (**Compare Figure 6 A and D**). Thus, the SEC profiles of SOF treated apo AI-reconstituted apo AI-null HDL and WT HDL are similar: both produce the smaller neo HDL and release LF apo AI.

Apo AI-null vs. WT HDL is More Stable: Several studies support the hypothesis that HDL is unstable because it resides in a kinetic trap.(*13, 15*) The faster reaction rate and greater extent of reaction, shown by higher I_{max} for WT vs. apo AI-null HDL, might be a manifestation of differences in HDL stability. We tested this hypothesis using chaotropic perturbation with GdmCl (**Figure 7**), which induces the release of LF apo AI and fusion of human HDL in a dose dependent way when used against human HDL.(*13, 15*) Given that apo AI-null HDL contains no apo AI, we compared the HDL on the basis of the shift in the elution volume of the fusion product. Previous chaotropic perturbation studies showed that WT mouse HDL and human HDL were similar (Compare **Figure 7 A—H** with previous data(*15*)). We observed that even at 0.5 M GdmCl, the main peak for WT HDL shifted to an earlier elution volume, corresponding to a larger particle, and a new peak appeared at 34 mL, corresponding to LF apo AI. As the GdmCl concentration increased, these changes continued: more LF apo AI was displaced from HDL, the amount of fused HDL(*13*) increased, and the main HDL peak (**Figure 7**, arrows) continued a linear shift ($m = -0.52 \pm 0.04$) to an earlier elution volume corresponding to larger particles (**Figure 7 Q**). Chaotropic perturbation of apo AI-null HDL also increased the size of the particle but at a much slower rate ($m = -0.17 \pm 0.04$). Thus, according to the ratios of the slopes of elution peak vs. molar concentration of GdmCl, apo AI-null HDL is ~3 times more stable than WT HDL.

Chaotropic Perturbation of Apo AI-Reconsituted Apo AI-null HDL Releases LF Apo AI: Human apo AI was incorporated into apo AI-null HDL as described above, incubated with various concentrations of GdmCl, and analyzed by SEC (**Figure 8**). These data show that at ≥1 M GdmCl, apo AI is released from apo AI-reconstituted apo AI-null HDL. This complements the SOF data of **Figure 6**, showing the restoration of normal HDL response to exogenous perturbants.

Discussion

Apo AI-null HDL is SOF Resistant In Vitro and In Vivo: Comparison of the SOF reaction vs. normal human and apo AI-deficient TLP showed the disappearance of a peak for HDL, the appearance of a CERM, and the formation of neo HDL (**Figures 1 and 3**). The amount of CERM formed from apo AI-deficient TLP is less than that formed from normal plasma TLP, an effect that we attribute to the much smaller amount of HDL available for conversion to CERM in the apo AI-deficient plasma. Comparison of the SOF reaction vs. human apo AI-deficient TLP and mouse apo AI-null HDL showed the disappearance of a peak for HDL, the appearance of a CERM, and the formation of neo HDL (**Figures 1 and 3**). Although there are differences between human and mouse apo AI and AII,(*28, 29*) most studies show that the latter apo is more lipophilic than the former.(*19, 30-32*) Thus, the apo AI-null mouse and its HDL are good but not perfect models for understanding the SOF reaction in the context of human apo AI-deficiency.

We directly tested the hypothesis that that the SOF reaction requires labile apo AI by measuring the reaction of SOF against HDL from apo AI-null mice. Although we found no requirement for apo AI, the in vitro rate and magnitude of opacification of apo AI-null HDL were respectively slower and smaller than that of WT HDL, and the in vivo rate and magnitude of cholesterol reduction in apo AI-null mice were diminished compared to WT (**Figures 2, 3**). For comparison, the scavenger receptor class B, type I-null mouse has elevated plasma total cholesterol (267 $\pm$ 12 mg/dL), and injection of SOF reduces the plasma cholesterol by 58% (unpublished data), suggesting that the magnitude of the SOF effect on plasma cholesterol is a function of the starting total plasma cholesterol. Another study showed that the SOF reaction rate increased with the concentration of apo AI-null HDL even though the rate constants were the same (unpublished data). Except for the release of LF apo AI, the protein compositions of the products of the reaction of SOF against apo AI-null and WT HDL were similar. Apo AI-null HDL was apo AII- and apo E-rich, and following the reaction most of these two apos remained with the neo HDL, although, as with WT, some apo E associated with the CERM (**Figure 3**).

Apo AI-null vs. human and mouse WT HDL, CERM, and Neo HDL Composition are Different: The size and compositions of HDL, neo HDL, and CERM from apo AI-null mice were different from their human and WT mouse counterparts. According to the SEC profile, apo AI-null mouse HDL is larger than human HDL, and, compared to human HDL, apo AI-null mouse HDL was PL- and CE-rich (+26% and +36% respectively) and protein-poor (-10%) (**Figure 4**). The major differences in the compositions of the SOF products formed from human and apo AI-null mouse HDL are due to the higher CE content of apo AI-null HDL and the failure of the SOF reaction against HDL to produce any LF apolipoproteins. The former is reflected in the higher CE content of the CERM formed from apo AI-null mouse HDL. The latter is reflected in a lower phospholipid content of apo AI-null mouse HDL vs. human HDL because additional PL must replace the surface protein, apo AI, which is lost during the reaction against human HDL. Furthermore, apo AI-null mouse neo HDL is more protein-rich than human neo HDL (**Figure 7**), even though the opposite is observed for the precursor HDL—human HDL is more protein-rich than apo AI-null HDL. We suggest that this difference lies in the observation that human, but not apo AI-null,

HDL loses nearly half of its protein, apo AI, during the SOF reaction. Similarly, the SOF reaction with WT mouse HDL displaces nearly half of the HDL-apo AI to the aqueous phase as a LF species.(*23*) Finally, we hypothesized that human neo HDL is more phospholipid-rich than apo AI-null neo HDL due to the retention of nearly all HDL protein on apo AI-null HDL, leaving less room for the other major surface component, phospholipids. This hypothesis is supported by the data of **Figure 4**, which shows 19 vs. 42% for mouse and human neo HDL respectively.

Apo AI-Null HDL is More Stable than WT HDL: The stability of HDL is determined, in part, by apolipoprotein composition and size, with apo AII and large size being associated with greater stability.(*15, 26*) We used chaotropic perturbation with GdmCl to test the hypothesis that the slower rate of disruption of HDL structure by SOF is due to the greater stability of apo AI-null vs. WT HDL. This test, (**Figure 7**), shows an increase in the size of apo AI-null and WT HDL but with different slopes, indicating different stabilities; the greater instability of WT HDL is distinguished by the release of LF apo AI, even at 0.5 M GdmCl. The greater stability of apo AI-null HDL would be expected to alter its functionality compared to WT mouse HDL.

Apo AI-null HDL, a Model for Nascent HDL? The chemistry of apo AI-null HDL is similar to what we observed for nascent apo AII-containing HDL secreted by hepatocytes.(*33, 34*) Although intrahepatic apo AII occurs on particles without apo AI, soon after secretion, plasma apo AII occurs on apo AI-containing particles, a finding that could occur through fusion of apo AI- and apo AII-containing HDL or by the transfer of LF apo AI to apo AII-containing HDL; our apo AI reconstitution data (**Figure 6**) supports the latter mechanism without necessarily excluding the former; most evidence supports the fusion mechanism.(*33, 35*) Thus, addition of apo AI to apo AI-null HDL simulates the remodeling of newly secreted hepatic HDL and restores a WT SOF product profile, i.e., the appearance of CERM, neo HDL, and LF apo AI.

Our studies addressed the hypothesis that apo AI is required for the SOF reaction against HDL by testing SOF's effects on apo AI-null HDL. These tests led to two conclusions. First, the reaction vs. apo AI-null HDL is slower and less profound than that vs. human HDL; thus, apo AI is not necessary for the reaction but in some way facilitates CERM formation. Second, according to chaotropic perturbation tests of HDL stability, apo AI-null HDL is more stable than WT mouse or human HDL (**Figure 7**), from which we conclude that the presence of the labile apo AI contributes to HDL instability and a more SOF-reactive particle. It is not clear whether HDL stability plays a role in atherogenesis, particularly considering that apo AI-null mice are atheroresistant.(*27*) Future studies could determine whether apo AI-null vs. native mouse or human HDL exhibits greater resistance to other HDL-modifying proteins, such as lipid-transfer proteins, lecithin-cholesterol acyltransferase (LCAT), and plasma lipases, or to cell surface receptors and how this affects HDL in vivo functionality.

Acknowledgements: We are grateful to Jennifer Connell, PhD who provided editorial assistance.

Funding Information: Supported by HL R01HL056865 from the National Institutes of Health.

References Cited

1. Castelli, W. P., Doyle, J. T., Gordon, T., Hames, C. G., Hjortland, M. C., Hulley, S. B., Kagan, A., and Zukel, W. J. (1977) HDL cholesterol and other lipids in coronary heart disease. The cooperative lipoprotein phenotyping study, *Circulation 55*, 767-772.
2. Williams, P. T., and Feldman, D. E. (2011) Prospective study of coronary heart disease vs. HDL2, HDL3, and other lipoproteins in Gofman's Livermore Cohort, *Atherosclerosis 214*, 196-202.
3. Frick, M. H., Elo, O., Haapa, K., Heinonen, O. P., Heinsalmi, P., Helo, P., Huttunen, J. K., Kaitaniemi, P., Koskinen, P., Manninen, V., and et al. (1987) Helsinki Heart Study: primary-prevention trial with gemfibrozil in middle-aged men with dyslipidemia. Safety of treatment, changes in risk factors, and incidence of coronary heart disease, *The New England journal of medicine 317*, 1237-1245.
4. Manninen, V., Elo, M. O., Frick, M. H., Haapa, K., Heinonen, O. P., Heinsalmi, P., Helo, P., Huttunen, J. K., Kaitaniemi, P., Koskinen, P., and et al. (1988) Lipid alterations and decline in the incidence of coronary heart disease in the Helsinki Heart Study, *JAMA : the journal of the American Medical Association 260*, 641-651.
5. Sung, K. C., Wild, S. H., and Byrne, C. D. (2013) Controlling for apolipoprotein A-I concentrations changes the inverse direction of the relationship between high HDL-C concentration and a measure of pre-clinical atherosclerosis, *Atherosclerosis 231*, 181-186.
6. Gursky, O., Mei, X., and Atkinson, D. (2012) The crystal structure of the C-terminal truncated apolipoprotein A-I sheds new light on amyloid formation by the N-terminal fragment, *Biochemistry 51*, 10-18.
7. Schaefer, E. J., Santos, R. D., and Asztalos, B. F. (2010) Marked HDL deficiency and premature coronary heart disease, *Current opinion in lipidology 21*, 289-297.
8. Santos, R. D., Schaefer, E. J., Asztalos, B. F., Polisecki, E., Wang, J., Hegele, R. A., Martinez, L. R., Miname, M. H., Rochitte, C. E., Da Luz, P. L., and Maranhao, R. C. (2008) Characterization of high density lipoprotein particles in familial apolipoprotein A-I deficiency, *Journal of lipid research 49*, 349-357.
9. Li, H., Reddick, R. L., and Maeda, N. (1993) Lack of apoA-I is not associated with increased susceptibility to atherosclerosis in mice, *Arteriosclerosis and thrombosis : a journal of vascular biology / American Heart Association 13*, 1814-1821.
10. Al-Sarraf, A., Al-Ghofaili, K., Sullivan, D. R., Wasan, K. M., Hegele, R., and Frohlich, J. (2010) Complete Apo AI deficiency in an Iraqi Mandaean family: case studies and review of the literature, *Journal of clinical lipidology 4*, 420-426.
11. Curtiss, L. K., Valenta, D. T., Hime, N. J., and Rye, K. A. (2006) What is so special about apolipoprotein AI in reverse cholesterol transport?, *Arteriosclerosis, thrombosis, and vascular biology 26*, 12-19.
12. Pownall, H. J., and Ehnholm, C. (2006) The unique role of apolipoprotein A-I in HDL remodeling and metabolism, *Current opinion in lipidology 17*, 209-213.
13. Mehta, R., Gantz, D. L., and Gursky, O. (2003) Human plasma high-density lipoproteins are stabilized by kinetic factors, *Journal of molecular biology 328*, 183-192.
14. Jayaraman, S., Gantz, D. L., and Gursky, O. (2005) Kinetic stabilization and fusion of apolipoprotein A-2:DMPC disks: comparison with apoA-1 and apoC-1, *Biophysical journal 88*, 2907-2918.
15. Pownall, H. J., Hosken, B. D., Gillard, B. K., Higgins, C. L., Lin, H. Y., and Massey, J. B. (2007) Speciation of human plasma high-density lipoprotein (HDL): HDL stability and apolipoprotein A-I partitioning, *Biochemistry 46*, 7449-7459.

16. Schwartz, G. G., Olsson, A. G., Abt, M., Ballantyne, C. M., Barter, P. J., Brumm, J., Chaitman, B. R., Holme, I. M., Kallend, D., Leiter, L. A., Leitersdorf, E., McMurray, J. J., Mundl, H., Nicholls, S. J., Shah, P. K., Tardif, J. C., Wright, R. S., and dal, O. I. (2012) Effects of dalcetrapib in patients with a recent acute coronary syndrome, *The New England journal of medicine 367*, 2089-2099.
17. Clay, M. A., Newnham, H. H., Forte, T. M., and Barter, P. I. (1992) Cholesteryl ester transfer protein and hepatic lipase activity promote shedding of apo A-I from HDL and subsequent formation of discoidal HDL, *Biochimica et biophysica acta 1124*, 52-58.
18. Silver, E. T., Scraba, D. G., and Ryan, R. O. (1990) Lipid transfer particle-induced transformation of human high density lipoprotein into apolipoprotein A-I-deficient low density particles, *The Journal of biological chemistry 265*, 22487-22492.
19. Liang, H. Q., Rye, K. A., and Barter, P. J. (1996) Remodelling of reconstituted high density lipoproteins by lecithin: cholesterol acyltransferase, *Journal of lipid research 37*, 1962-1970.
20. Rao, R., Albers, J. J., Wolfbauer, G., and Pownall, H. J. (1997) Molecular and macromolecular specificity of human plasma phospholipid transfer protein, *Biochemistry 36*, 3645-3653.
21. Lusa, S., Jauhiainen, M., Metso, J., Somerharju, P., and Ehnholm, C. (1996) The mechanism of human plasma phospholipid transfer protein-induced enlargement of high-density lipoprotein particles: evidence for particle fusion, *The Biochemical journal 313 (Pt 1)*, 275-282.
22. Gillard, B. K., Courtney, H. S., Massey, J. B., and Pownall, H. J. (2007) Serum opacity factor unmasks human plasma high-density lipoprotein instability via selective delipidation and apolipoprotein A-I desorption, *Biochemistry 46*, 12968-12978.
23. Rosales, C., Tang, D., Gillard, B. K., Courtney, H. S., and Pownall, H. J. (2011) Apolipoprotein E mediates enhanced plasma high-density lipoprotein cholesterol clearance by low-dose streptococcal serum opacity factor via hepatic low-density lipoprotein receptors in vivo, *Arteriosclerosis, thrombosis, and vascular biology 31*, 1834-1841.
24. Han, M., Gillard, B. K., Courtney, H. S., Ward, K., Rosales, C., Khant, H., Ludtke, S. J., and Pownall, H. J. (2009) Disruption of human plasma high-density lipoproteins by streptococcal serum opacity factor requires labile apolipoprotein A-I, *Biochemistry 48*, 1481-1487.
25. Courtney, H. S., Hasty, D. L., Li, Y., Chiang, H. C., Thacker, J. L., and Dale, J. B. (1999) Serum opacity factor is a major fibronectin-binding protein and a virulence determinant of M type 2 Streptococcus pyogenes, *Molecular microbiology 32*, 89-98.
26. Rosales, C., Gillard, B. K., Courtney, H. S., Blanco-Vaca, F., and Pownall, H. J. (2009) Apolipoprotein modulation of streptococcal serum opacity factor activity against human plasma high-density lipoproteins, *Biochemistry 48*, 8070-8076.
27. Williamson, R., Lee, D., Hagaman, J., and Maeda, N. (1992) Marked reduction of high density lipoprotein cholesterol in mice genetically modified to lack apolipoprotein A-I, *Proceedings of the National Academy of Sciences of the United States of America 89*, 7134-7138.
28. Lyssenko, N. N., Hata, M., Dhanasekaran, P., Nickel, M., Nguyen, D., Chetty, P. S., Saito, H., Lund-Katz, S., and Phillips, M. C. (2012) Influence of C-terminal alpha-helix hydrophobicity and aromatic amino acid content on apolipoprotein A-I functionality, *Biochimica et biophysica acta 1821*, 456-463.
29. Alexander, E. T., Vedhachalam, C., Sankaranarayanan, S., de la Llera-Moya, M., Rothblat, G. H., Rader, D. J., and Phillips, M. C. (2011) Influence of apolipoprotein A-I domain structure on macrophage reverse cholesterol transport in mice, *Arteriosclerosis, thrombosis, and vascular biology 31*, 320-327.
30. Lagocki, P. A., and Scanu, A. M. (1980) In vitro modulation of the apolipoprotein composition of high density lipoprotein. Displacement of apolipoprotein A-I from high density lipoprotein by apolipoprotein A-II, *The Journal of biological chemistry 255*, 3701-3706.
31. Edelstein, C., Halari, M., and Scanu, A. M. (1982) On the mechanism of the displacement of apolipoprotein A-I by apolipoprotein A-II from the high density lipoprotein surface. Effect of

concentration and molecular forms of apolipoprotein A-II, *The Journal of biological chemistry 257*, 7189-7195.
32. Kunitake, S. T., and Kane, J. P. (1982) Factors affecting the integrity of high density lipoproteins in the ultracentrifuge, *Journal of lipid research 23*, 936-940.
33. Gillard, B. K., Lin, H. Y., Massey, J. B., and Pownall, H. J. (2009) Apolipoproteins A-I, A-II and E are independently distributed among intracellular and newly secreted HDL of human hepatoma cells, *Biochimica et biophysica acta 1791*, 1125-1132.
34. Chisholm, J. W., Burleson, E. R., Shelness, G. S., and Parks, J. S. (2002) ApoA-I secretion from HepG2 cells: evidence for the secretion of both lipid-poor apoA-I and intracellularly assembled nascent HDL, *Journal of lipid research 43*, 36-44.
35. Clay, M. A., Pyle, D. H., Rye, K. A., and Barter, P. J. (2000) Formation of spherical, reconstituted high density lipoproteins containing both apolipoproteins A-I and A-II is mediated by lecithin:cholesterol acyltransferase, *The Journal of biological chemistry 275*, 9019-9025.
36. Gillard, B. K., Rosales, C., Pillai, B. K., Lin, H. Y., Courtney, H. S., and Pownall, H. J. (2010) Streptococcal serum opacity factor increases the rate of hepatocyte uptake of human plasma high-density lipoprotein cholesterol, *Biochemistry 49*, 9866-9873.

Figure Legends

Figure 1: Effects of SOF on the SEC of plasma TLP from an apo AI-deficient patient. A, Human plasma TLP. B, SOF + Human plasma TLP (Reproduced from Gillard et al).(*36*) C, Human apo AI-deficient TLP. D, SOF + Human apo AI-deficient TLP. Dashed curves (CERM) are the difference between the curves in A and B and C and D.

Figure 2: Kinetic curves for the change in total plasma cholesterol following injection of saline (●) and SOF (O) into apo AI-null C57Bl/6 mice. The curve for saline injection was fitted to a first order linear polynomial. The curve for SOF injection into apo AI-null mice was fitted to a third-order hyperbolic decay. Plotted values are the means ± SEM. The asterisks indicate that points for SOF injection are significantly different ($p < 0.05$) from saline injection and from $t = 0$ for SOF injection.

Figure 3: SEC of apo AI-null mouse HDL before and after reaction vs. SOF. SEC of apo AI-null mouse HDL (A). SEC of the products of the reaction of SOF against apo AI-null mouse HDL (B). SDS-PAGE of the fractions collected from the SEC of reaction products and visualized by Coomassie blue staining (C) and immunobotting with antibodies against apo AI (D), apo E (E), and apo AII (F).

Figure 4: Compositions of HDL, CERM, and neo HDL from apo AI-null mice. HDL (1.1 mg/mL in 0.8 mL) was incubated with 3 μg SOF at 37 °C in Tris-buffered saline overnight. The density of the reaction mixture was adjusted to 1.1 g/mL by addition of KBr and overlaid with ~7 mL d = 1.006 g/mL. The CERM was floated away from the neo HDL by centrifugation (48 h @ 40,000 rpm, Beckman SW 40 rotor). The horizontal lines in each bar are the compositions of the corresponding human lipoproteins.(*22*)

Figure 5: In vitro kinetics of the SOF reaction vs. HDL from WT and apo AI-null mice. HDL (100 μg/mL protein) was pre-equilibrated to 37 °C in a fluorescence cell in the sample chamber of the fluorimeter for 10 minutes, after which SOF (0.05 μg/mL) was added and the right-angle light scattering at 325 nm monitored. Upper curves: WT HDL; lower curves: apo AI-null HDL. Red lines are data points; black lines are the fitted data from which the I_{max} and k values were obtained.

Figure 6: Effects of apo AI-addition on SOF activity vs. apo AI-null HDL. SEC profiles of human apo AI (A), 0.5 mg apo AI-null HDL (B), 0.25 human apo AI + apo AI-null HDL (C), human apo AI + apo AI-null HDL + SOF (D).

Figure 7: Chaotropic perturbation of HDL from WT and apo AI-null mice by GdmCl. HDL, Tris-buffered saline, and GdmCl were combined to give a final HDL-protein concentration of 0.11 mg/mL and various concentrations of GdmCl, indicated on each panel (A and B), and were incubated at room temperature for 22 hours, after which the samples were analyzed by SEC. Elution volume of the GdmCl fusion product (arrowheads) versus GdmCl molar concentration (C).

Figure 8: Effects of apo AI-addition on apo AI-null HDL stability to chaotropic perturbation. Graded concentrations of GdmCl were added to apo AI-null HDL that was pre-incubated with human apo AI, and products were analyzed by SEC. GdmCl concentrations are as indicated in each panel. The elution volume for LF apo AI is indicated by the vertical dashed gray line.

Figure 1

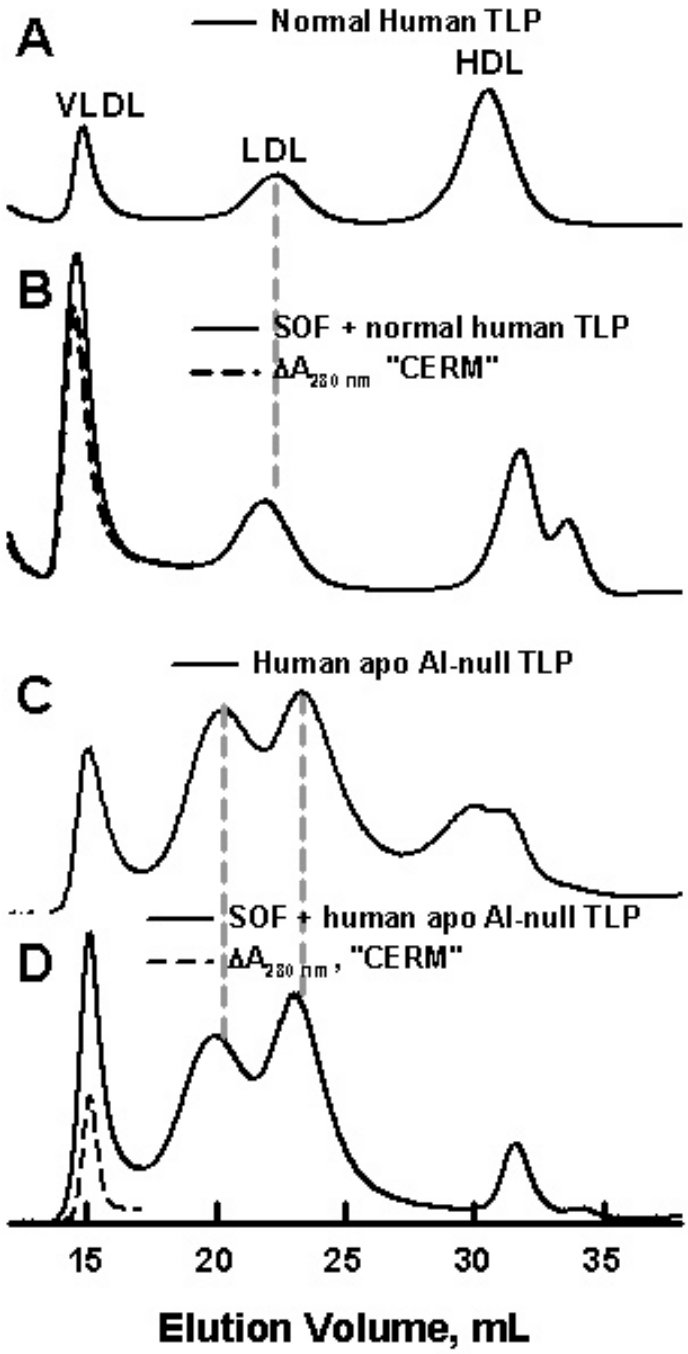
A
Normal Human TLP
HDL
VLDL
LDL
B
SOF + normal human TLP
ΔA280 nm "CERM"
C
Human apo AI-null TLP
SOF + human apo AI-null TLP
D
ΔA280 nm, "CERM"
15
20
25
30
35
Elution Volume, mL

Figure 2

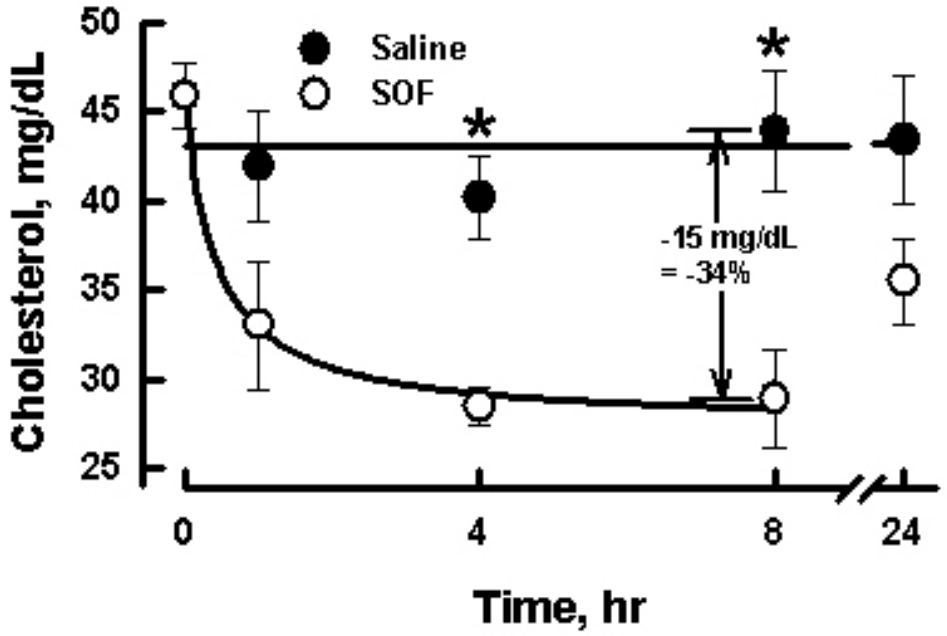
Cholesterol, mg/dL
50
45
40
35
30
25
Saline
SOF
*
*
-15 mg/dL
= -34%
0
4
8
24
Time, hr

Figure 3

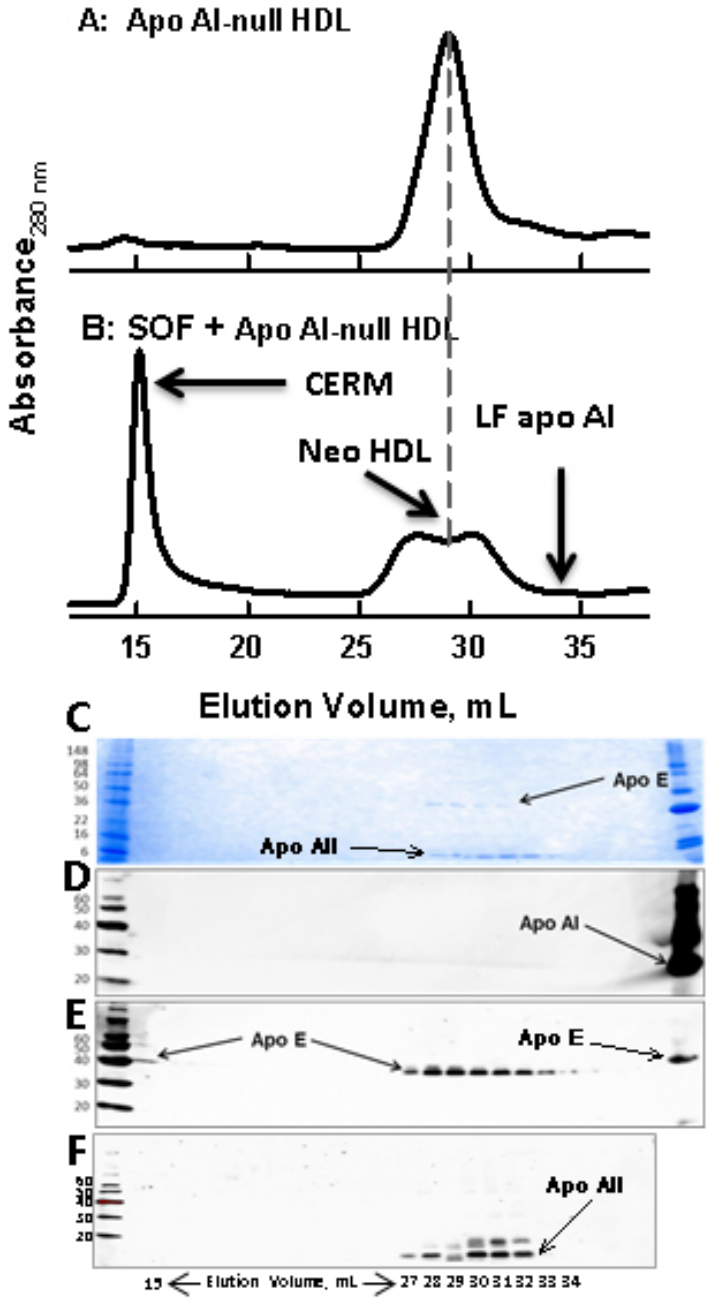
A: Apo AI-null HDL
Absorbance280 nm
B: SOF + Apo AI-null HDL
CERM
LF apo AI
Neo HDL
15
20
25
30
35
Elution Volume, mL
C
Apo E
Apo AII
D
Apo AI
E
Apo E
Apo E
F
Apo AII
15 Elution Volume, mL 27 28 29 30 31 32 33 34

Figure 4

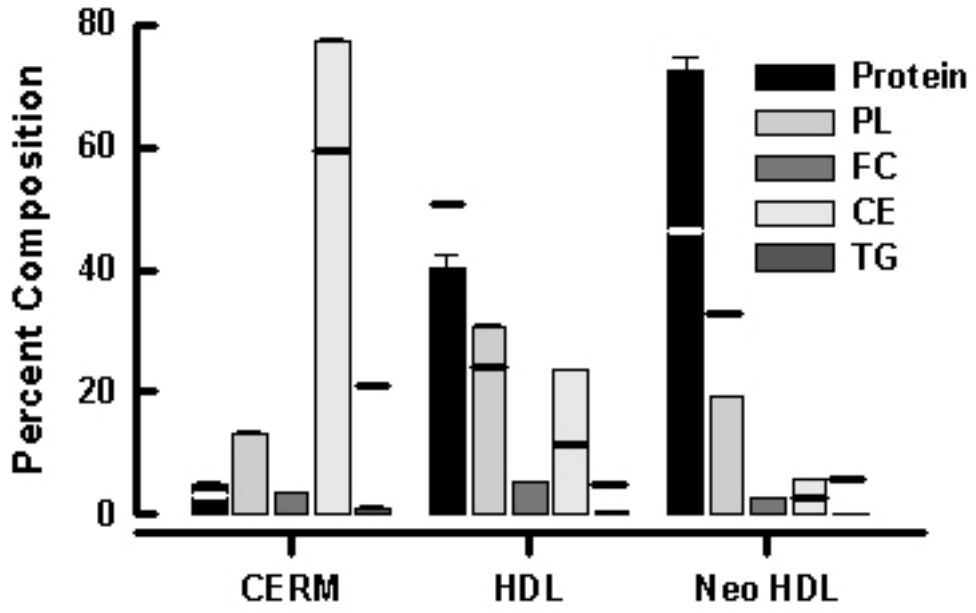
Percent Composition
80
60
40
20
0
Protein
PL
FC
CE
TG
CERM
HDL
Neo HDL

Figure 5

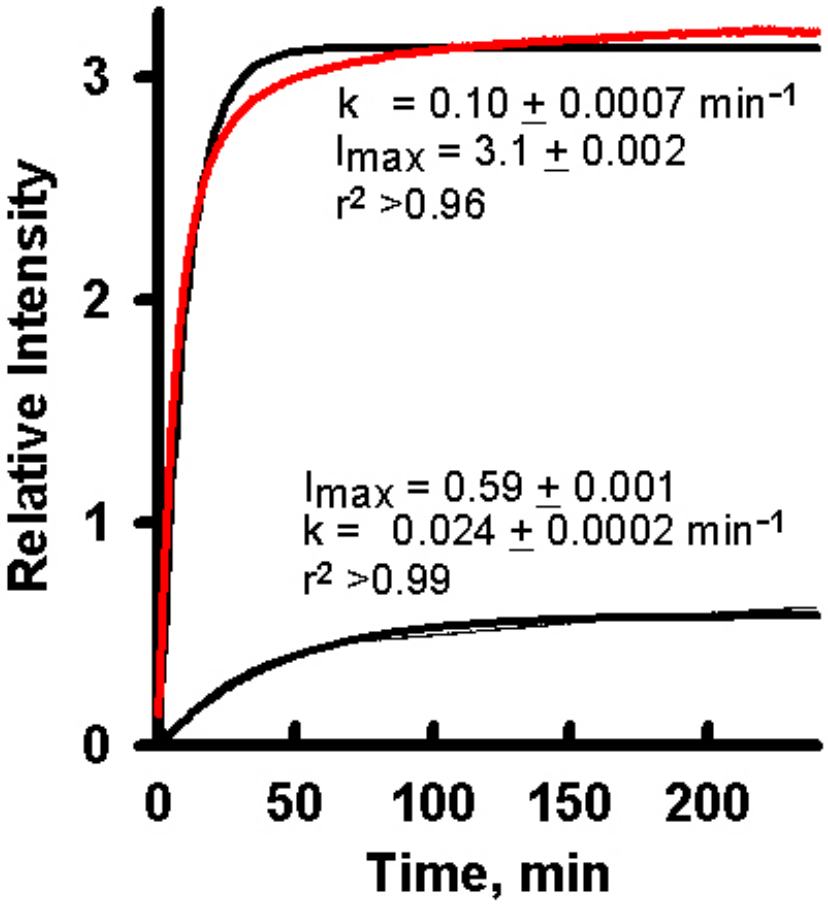
Relative Intensity
3
2
1
0
k = 0.10 ± 0.0007 min-1
Imax = 3.1 ± 0.002
r2 >0.96
Imax = 0.59 ± 0.001
k = 0.024 ± 0.0002 min-1
r2 >0.99
0
50
100
150
200
Time, min

Figure 6

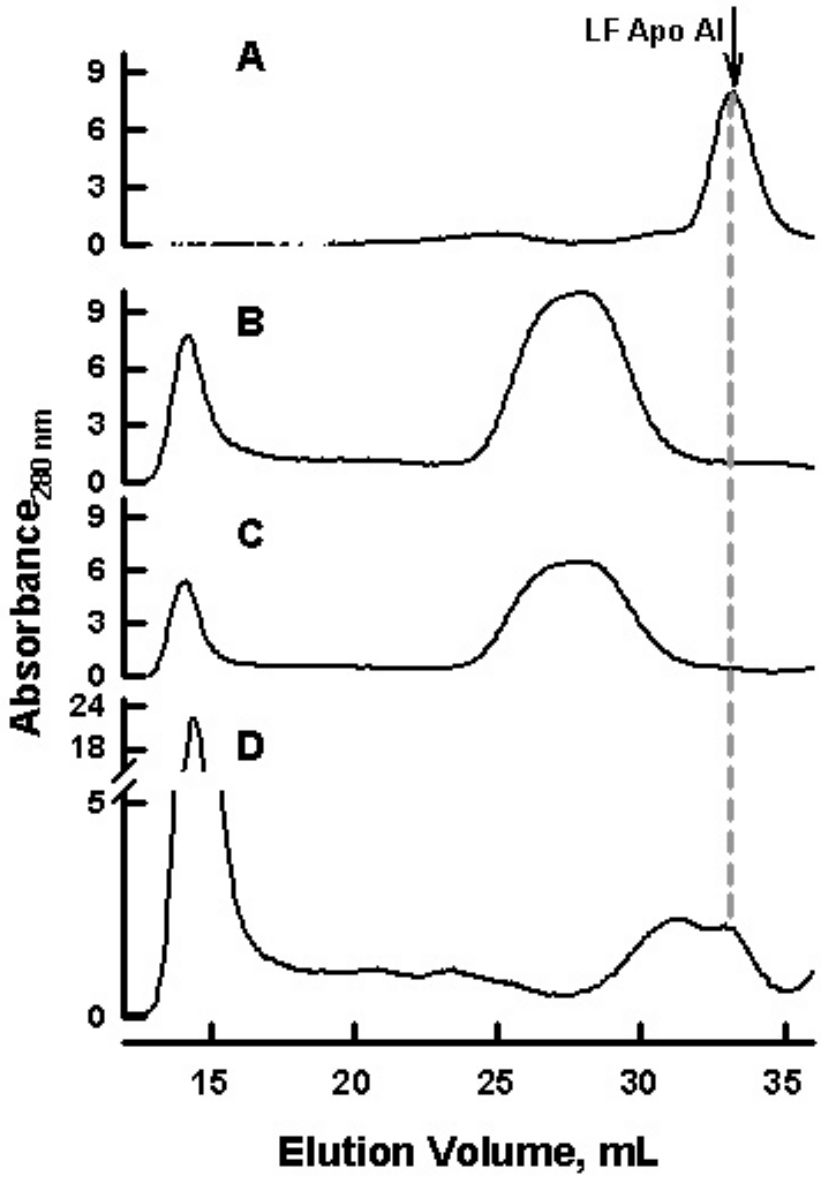
LF Apo AI
A
B
C
D
9
6
3
0
24
18
5
Absorbance280 nm
15
20
25
30
35
Elution Volume, mL

Figure 7

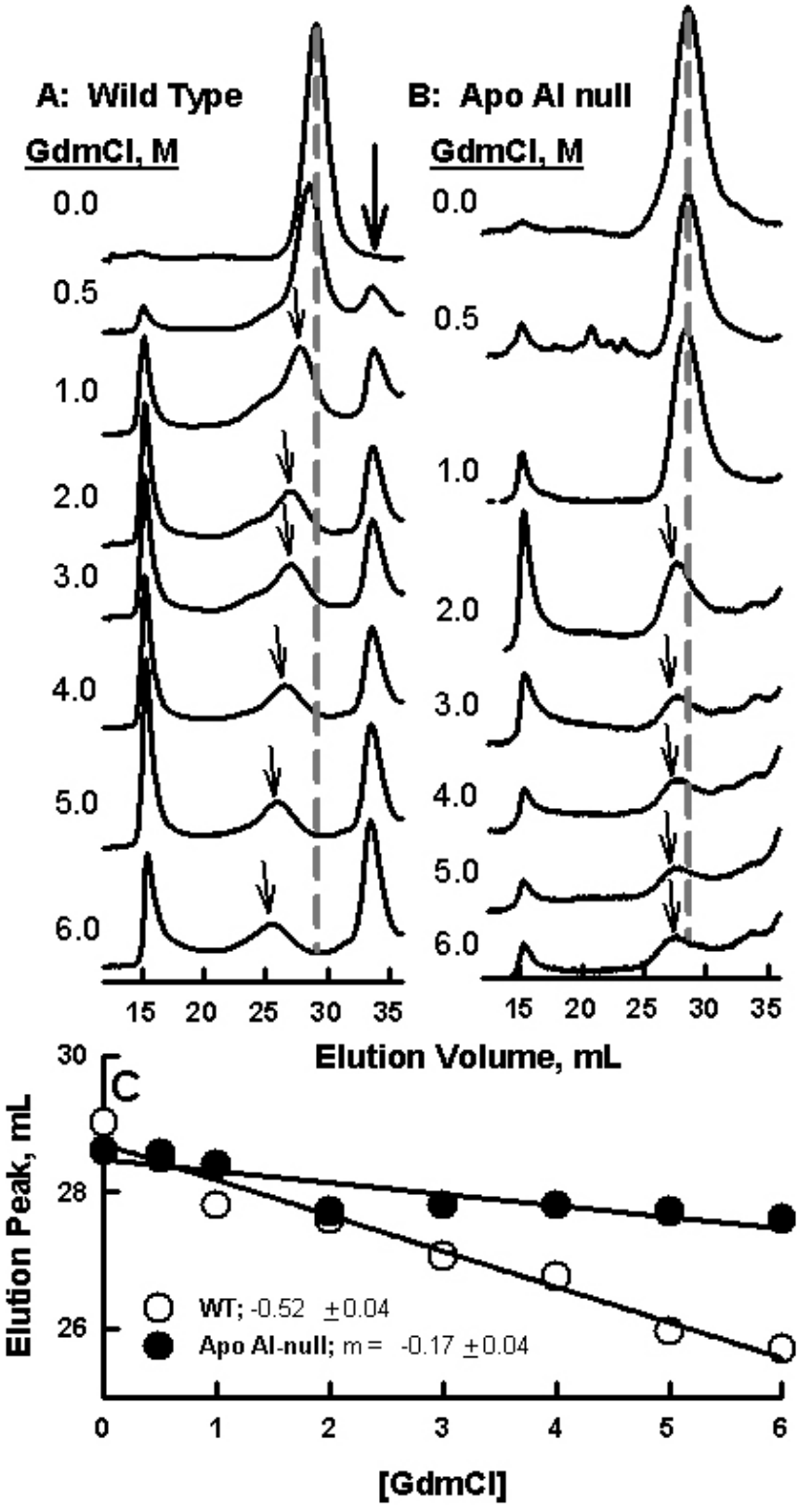
A: Wild Type
GdmCl, M
0.0
0.5
1.0
2.0
3.0
4.0
5.0
6.0
B: Apo AI null
GdmCl, M
0.0
0.5
1.0
2.0
3.0
4.0
5.0
6.0
15 20 25 30 35
15 20 25 30 35
Elution Volume, mL
C
Elution Peak, mL
30
28
26
WT; -0.52 ±0.04
Apo AI-null; m = -0.17 ±0.04
0 1 2 3 4 5 6
[GdmCl]

Figure 8

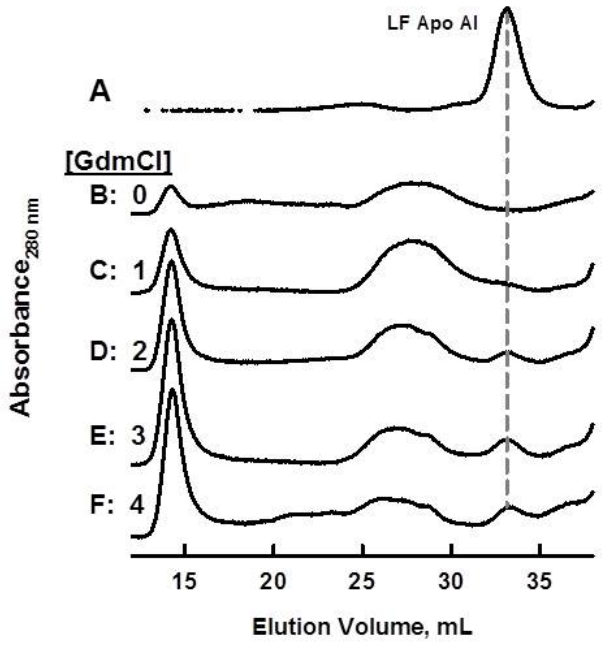
LF Apo AI
A
[GdmCl]
B: 0
C: 1
D: 2
E: 3
F: 4
Absorbance280 nm
15
20
25
30
35
Elution Volume, mL

Table of Contents Graphic